

Behavior of cloud base height from ceilometer measurements

By M. Costa-Surós^{1*}, J. Calbó¹, J.A. González¹, J. Martin-Vide²

¹Group of Environmental Physics, Physics Department, University of Girona (Spain)

²Group of Climatology, Department of Physical Geography, University of Barcelona (Spain)

Atmospheric Research

February, 2013

*Corresponding author.

e-mail: montse.costa@udg.edu

ABSTRACT

Given the importance of clouds in the climate, and the difficulty in determining their behavior and their contribution to climate change, there is a need for improvement of methods for automatic and continuous description of cloud characteristics. Ceilometers constitute a priori a reliable instrumental method for sounding the atmosphere and describing cloudiness, specifically cloud base height (CBH), cloud cover, and even cloud vertical structure. In the present study, the behavior of CBH at different time scales has been investigated at Girona (Spain) including a statistical analysis of the frequency distributions of CBH. The study covers four years (2007-2010) of high resolution (both in time and in the vertical direction) ceilometer measurements. At this location, ceilometer measurements reveal a seasonal cycle, with important differences between “extreme” seasons (winter and summer) and the “transition” seasons (spring and autumn). Summer months in general and July in particular behave quite differently than other periods in the year, both regarding the presence of clouds (with a minimum cloud occurrence of about 20-30%) and the distribution of CBH (with more than 25% of clouds having CBH around 1400 m and 80% of clouds with CBH lower than 3000 m). The distributions of CBH are explained on the basis of some atmospheric situations that generate clouds, in particular conditions that produce the large number of low level clouds found.

1. Introduction

Clouds are a key factor among the processes that drive the climate. Their capability to affect the shortwave and longwave components of radiative forcing (about ten times as large as those for carbon dioxide doubling) leads them to play a significant role as a climate feedback mechanism (Ramanathan *et al.* 1989; Salazar and Poveda, 2009). It is well known, however, the difficulty of determining how clouds contribute to climate change, due to the complexity of the processes involved, the vast amount of information needed, including spatial distribution, and the uncertainty associated with the available data (see Solomon *et al.*, 2007; Heintzenberg and Charlson, 2009; and, as a review, Wielicki *et al.*, 1995). There is, in consequence, a general need for improvement of automatic cloud observation and continuous cloud description for climatological issues. Specifically, more quantitative information is needed about cloud characteristics, behavior, interaction, and processes in which clouds take part.

The high temporal and spatial variability of clouds creates difficulties for their quantitative observation. In general, surface weather observations provide total cloud cover and cloud amount by morphological type, so frequency distributions of occurrence and co-occurrence of different cloud types may be derived. However, surface observers have difficulties identifying altostratus/altocumulus and cirrus clouds reliably, particularly at night or when lower clouds are present. In addition, surface observations do not provide any information on cloud-top height or optical thickness (Poore *et al.*, 1995). These and other difficulties result in a limited number of climatic studies on cloudiness, especially when compared with studies of other variables such as temperature or precipitation. There are, however, a number of notable exceptions: for example, Warren *et al.* (2007) developed a global climatology of clouds; at continental

scale we can mention the works by Henderson-Sellers (1992) for Europe, Dai *et al.* (2006) for the USA, Kaiser (2000) for China, and Sun and Groisman (2000) for the former Soviet Union; finally Calbó and Sanchez-Lorenzo (2009) presented a cloud climatology for the Iberian Peninsula.

Besides the temporal and spatial distribution of cloudiness, cloud base and top heights (which are linked to cloud type) are important characteristics in order to describe the impact of clouds in a changing climate (Ramanathan *et al.* 1989; Zelinka and Hartmann, 2010). Several approaches are possible for observing and investigating such characteristics; these approaches may be classified in ground based instrumentation, satellite-based observation, and meteorological model simulation. Forsythe *et al.* (2000) and references therein summarize the research oriented to retrieve cloud type and cloud base height; further discussion about the advantages and limitations of satellite and surface observations can be found in Warren and Hahn (2002).

Regarding satellite-based observation and description of clouds, the International Satellite Cloud Climatology Project (ISCCP) reports global distributions of cloud amount, cloud-top temperature/pressure, and optical thickness, among other variables (Rossow and Schiffer, 1991). On the other hand, the Nimbus-7 cloud climatology provides information on cloud altitude distributions and cloud amount (Hwang *et al.* 1988). Note that the partially obscured view of low-level clouds and the difficulties in estimating the heights of thinner cirrus lead to large uncertainties in determining the vertical distribution of cloud layers from satellite-based imagery (Poore *et al.*, 1995). More recently, however, new instruments onboard of satellites are providing details about the cloud vertical structure. In particular, active sensors such as the Cloud

Profiling Radar (CPR) on *CloudSat* and the Cloud–Aerosol Lidar with Orthogonal Polarization (CALIOP) aboard *CALIPSO* (*Cloud-Aerosol Lidar and Infrared Pathfinder Satellite Observation*) satellites are achieving notable results regarding the addition of a vertical dimension to traditional satellite images. Nevertheless, because the repeat time for any particular location is very large, the time resolution of such observations is low (L'Ecuyer and Jiang, 2010; de Leeuw *et al.*, 2012.). In this sense, Kotarba (2009) discussed the matching between satellite and surface-based observations of clouds, and proved that surface data collected within 30 min before or after a pass by any satellite sensor can be used as a good approximation of exactly matched observations.

As for the treatment of cloud formation and cloud characteristics by meteorological models, Willén *et al.* (2005) tested several general circulation models and found that they overestimate the occurrences of small cloud fractions and underestimate the occurrences of clear-sky and overcast. In fact, clouds occur more frequently in the models, but with less amounts when present. In addition, models tend to produce lower cloud base heights when compared with measurements by lidars. For example, Van Lipzig *et al.* (2006) and Schroeder *et al.* (2006) comment on the BALTEX Bridge Campaigns (BBC) measurements and state that this data can be used to investigate whether ‘state-of-the-art’ atmospheric models are capable of adequately representing clouds. Moreover, Hogan *et al.* (2009) found that models tend to be least skillful at predicting the timing and placement of boundary-layer clouds and most skillful at predicting mid-level clouds. Recently, Probst *et al.* (2012) compared global and zonal cloud cover fraction for total cloudiness from the ISCCP D2 dataset to the same quantities produced by 21 climate models, and found that most models underestimate the yearly averaged values of cloudiness over all the analyzed areas. Similarly, an assessment of models based on ground based instruments is addressed by

the Cloudnet Project. Specifically, the aim of this project is to provide a systematic evaluation of clouds in forecast models (Illingworth *et al.*, 2007) by comparing with the cloud fraction derived from long-term radar, lidar and microwave radiometer.

As far as ground-based instrumentation is concerned, ceilometers are the most common instruments mainly devoted to determining the cloud base height (CBH). Traditionally, their importance has always been closely linked to the needs of aviation (Holejko and Nowak, 2000). Thus, development of an automated ceilometer system for measuring cloud amounts and CBH was required to meet the needs of the increasing volume of aviation traffic and to replace systems based on visual observations (Mancuso *et al.*, 1971). The current instruments are based on LIDAR (Light Detection And Ranging) technology, incorporating a diode laser that emits short light pulses focused to a collimated beam and transmitted into the atmosphere. The altitude profile of the backscattered light allows determining CBH, which is usually defined as the height at which the ceilometer signal returns its maximum value (Eberhard, 1986); sometimes, the highest backscatter signal is not coming from the base of the cloud (e.g. when there is precipitation), a fact that is taken into account by the most advanced algorithms that treat the signal. Other information can be derived from the backscatter signal such as the convective mixing height (Münkel *et al.*, 2007).

To obtain a more complete description of cloud fields, however, a set of complementary instruments is required. As said above, clouds may occur in distinct layers or in layers that merge together, and layers can conceal and obscure each other. In particular, typical ceilometers provide good vertical resolution of CBH and higher temporal resolution than visual or satellite observations, but they can hardly give information on the horizontal extent of the cloud layers, given their narrow field-of-

view. In addition, they only report cloud bases up to some cutoff height, beyond which no clouds are reported (Forsythe *et al.*, 2000). Consequently, Moran *et al.* (1998) affirm that other instruments that penetrate the cloud such as the millimeter-wave cloud radar (MMCR) may be combined with simultaneous measurements by radiometers and lidars to estimate several cloud properties. Similarly, Hogan *et al.* (2003) investigate the frequency of occurrence of clouds (derived from lidar, radar, microwave radiometer observations) as a function of temperature obtained from a weather model. Forsythe *et al.* (2000) note that the latter instruments do not usually have the spatial or temporal coverage necessary to make them useful for many applications; nowadays, however, these instruments can be operated with a high temporal resolution as in the Atmospheric Radiation Measurement program (ARM). Moreover, ARM issues a value added product called ARSCL (Active Remotely-Sensed Cloud Locations) which integrates ceilometer, Micropulse Lidar, and MMCR measurements to produce time series of vertical distributions of cloud hydrometeors (Clothiaux *et al.*, 2000). An example of the use of this ARM instrumentation is found in Mace and Benson (2008) where data collected over 8 years were used to examine the statistics of cloud occurrence and the influence of clouds on the radiation budget.

There are other methods to investigate the cloud vertical structure. In particular, vertical profiles from radiosondes have been used by several authors to describe it (e.g. Poore *et al.*, 1995; Wang and Rossow, 1995; Wang *et al.*, 1999; Wang *et al.*, 2000). An example of the use of radiosondes combined with satellites (MODIS) was provided by Jin *et al.* (2007), which explored the detection of cloud vertical structures over the Arctic.

A comparison between different types of ground-based sensors used to derive macroscopic cloud data such as cloud cover and CBH is presented in Feister *et al.* (2010). In another recent study, Ebell *et al.* (2011) derived cloud statistics by using the ARM Mobile Facility, the Cloudnet database, and in support of the Convective and Orographically-induced Precipitation Study (COPS), for a low-mountain site in Germany. In summary, it is usually accepted that cloud characteristics obtained from satellite and from the ground (either subjective or instrumental observations) are complementary to each other to acquire a comprehensive understanding of extension, height, and structure of clouds.

Regarding the CBH specifically, inter-comparison of measurements by laser ceilometers from different manufacturers have been carried out several times. For example, during the WMO International Ceilometer Intercomparison (Jones *et al.*, 1988) several designs of ceilometers were inter-compared and also other tests were made by comparing with rotating-beam ceilometers (RBC) and pilot-balloon observations. Some early comparisons between RBC and newly developed laser ceilometers indicated that RBC had a superior performance during moderate rain. Recently, Martucci *et al.* (2010) studied twelve cases of multilayer CBH retrievals from two ceilometers (Vaisala CL31 and Jenoptik CHM15K) from September to December 2008 in Ireland and they suggested applying an independent algorithm to both ceilometer backscatter signals to provide more accurate estimates of the CBH in both simple and complex cloud patterns. Nevertheless, the WMO still recognizes that, using current technology, laser ceilometers provide the most accurate, reliable and efficient means of measuring CBH from the ground when compared with alternative equipment (WMO, 2008).

Within the general goal of obtaining insight about the behavior of cloudiness, the specific aim of this study is acquiring a deep knowledge (including behavior at different time scales) about the CBH measured from the surface with a ceilometer. Details on the instrument used and the data acquired are given in Section 2. Then in Section 3 some results about cloud occurrence, cloud vertical structure and CBH distributions of the whole data set are analyzed. Furthermore, a detailed statistical analysis of the CBH frequency distributions is performed in monthly and seasonal basis. These distributions are compared with previous results found in the literature concerning CBH behavior, mainly the works by Poore *et al.* (1995, hereinafter PWR95), Wang and Rossow (1995, WR95), Wang *et al.* (1999, WRUR99), and Wang *et al.* (2000, WRZ00). Moreover, some specific atmospheric situations are described, adding some insight into the frequency distributions of CBH. Finally, results are summarized in Section 4, where some conclusions are derived, and hints for further work are given.

2. Data: Ceilometer measurements

The Environmental Physics Group of the University of Girona maintains, since December 2006, a laser ceilometer, model *CL-31* from *Vaisala*, which is installed on the roof of a building of the Escola Politècnica Superior ($41^{\circ}57'48''\text{N}$, $2^{\circ}49'52''\text{E}$, 110 m a.s.l.), in Girona (NE of the Iberian Peninsula). This ceilometer takes backscattering profiles up to 7620 m, from which the CBH for up to three cloud layers are retrieved by the algorithm provided by *Vaisala*. The central wavelength of the emitted light is about 910 nm, the vertical resolution has been programmed to 10 m and backscatter profiles are stored every 12 seconds. This instrument, in fact, has become a standard both for operational purposes (in particular at airports) and for research goals (it is a common instrument at ARM and Baseline Surface Radiation Network measurement sites). Other radiation and meteorological sensors, as well as an upwards looking hemispherical camera operating continuously (Long *et al.*, 2006) are installed at the same place.

A period of 4 years, from January 2007 to December 2010, has been analyzed. From the total possible measurements in this period, nearly the 92% is available. In fact, 17 months out of the 48 have 100% of data, and for most months there is more than 80% of the possible data to do the statistical analysis. Exceptions are May and June 2010, which present lower percentages of availability (54% and 45% respectively) because the ceilometer was in maintenance and calibration service, and July and August 2010 (60% and 68%) when power faults in the building caused by thunderstorm episodes resulted in some missing data. Since the amount of available data for these four months is still enough to make statistical statements, we have applied the same data treatment. Despite the relatively short period (4 years), the high frequency of measurements (12 s) results in a very large dataset with more than 9.5 million records.

3. Results

3.1 Cloud occurrence

Here, we define *cloud occurrence* as the ratio between the number of registers with detected clouds (i.e. at least one CBH value) with respect to the total available records. Cloud occurrence is used here as an estimator of the cloud cover, which is a quantitative descriptor of cloudiness. This definition has also been used by PWR95, WR95, WRUR99 and WRZ00, where cloud layers derived mainly from radiosonde profiles are reported and analyzed. From the ceilometer data we have first obtained monthly estimations of cloud occurrence in percentage (Figure 1). Despite the year to year variability, some common features can be noted: most years follow a similar evolution, including a clear summer minimum (centered in July) (Figure 1a). However, missing data in May-August 2010 might have affected the cloud occurrence values. In particular, we cannot discard that the absolute minimum in July 2010 be linked to the lost data precisely during cloudy situations (note that power faults due to thunderstorms produced the instrument failure).

Figure 1b shows the average of these four years of monthly cloud occurrence and the 1973-2003 cloud cover mean obtained from visual observations at Girona Airport (a few kilometers from the ceilometer site) processed by the same methodology as in Llach and Calbó (2004): monthly means in tenths are built from three daily observations (at 7h, 13h and 18h). Although it is unrealistic to expect complete similarity between the observer and any instrumental output (Boers *et al.*, 2010) both evolutions agree well, showing a mean cloudiness around 40-50% along the year, except for the summer period, when the July minimum reaches around 30%. According

with Boers *et al.* (2010) this agreement between monthly means may be hiding important differences in the distributions of cloud occurrence as compared to the human observations. Note, however, that the monthly cloud occurrence detected by the ceilometer is lower than the cloud cover from visual observations, all the year long, except in the winter season, that breaks this trend. We attribute this underestimation to the limited vertical range of detection (7620 m). Of course, another reason for the mismatch between both series of data is that they correspond to different temporal periods. Nevertheless, the ceilometer cloud occurrence lies within the interannual variability described by the standard deviation of the monthly values.

Moreover, Figure 1c shows that the cloud occurrence detected with the ceilometer at Girona is also consistent with the annual and seasonal total cloud cover (TCC) that can be derived from a climatic description of cloudiness in the Iberian Peninsula (Calbó and Sanchez-Lorenzo, 2009). This latter study was limited to the 1983-2002 period to allow comparing results from three different sources of data: the International Satellite Cloud Climatology Project (ISCCP) D2 data, the gridded data (TS 2.1) from the Climate Research Unit (CRU), and the European Centre for Medium-Range Weather Forecasts (ECMWF) Re-Analyses data (ERA-40). Results indicated that, in the Iberian Peninsula, the mean annual cloudiness ranges from 35 to 65% of fractional sky cover, depending on location and on data source. Seasonal evolution showed a very clear minimum of cloudiness that appears in summer and a maximum in winter. A similar behavior was also found by Rossow *et al.* (2005) regarding cloud amounts at these latitudes inferred from satellites (ISCCP) and radiosonde profiles. Some differences appeared among the three sources, probably due to the higher sensitivity of satellite observations to cirrus clouds, the underestimation of high clouds due to the obscuring effect in surface observations, and the satellite overestimation of

low-level broken or scattered clouds (Calbó and Sánchez-Lorenzo, 2009). Thus, Figure 1c shows that seasonal cloud occurrence for Girona estimated from ceilometer measurements agree quite well with TCC values from the ERA dataset, and particularly in regards of the summer minimum.

Therefore, the estimated values of cloud cover from the ceilometer data (i.e., cloud occurrence) seem reasonable (although slightly lower) when compared either with visual observations taken at Girona airport or with the regional climatology based on surface and satellite observations. This is a notable fact, specially if one considers that this device has a very limited field of view, can hardly detect high clouds, the shortness of the treated period (4 years), and the simplicity of the cloud cover estimation. Therefore, when looking at long time series, the narrow field of view is partially compensated: it can be assumed that clouds are advected over the ceilometer so a representative sample of the 2-D cloud field is obtained in most, but not all, cases.

3.2 Cloud vertical structure

Ceilometer measurements allow obtaining information on the vertical structure of the cloud field (although cloud top heights cannot be derived straightforwardly). For the 4-year period studied, the ceilometer detected a single cloud layer in 89.7% of the cases, whereas 9.4% were 2-layered systems, and 0.9% were 3-layered systems (relative to the number of cases where some cloud was detected; cases labeled as full or partial obscuration –usually due to heavy fog or precipitation–, when no cloud base is detected, have not been included). In principle, the frequency of multilayered cases is expected to be underestimated by the ceilometer since high clouds may often be occulted by the

lower layers. Accordingly, from visual observations at Girona Airport (1973-2003), following SYNOP observation criteria, 46% of observations contain cloud types belonging to two different levels (low and middle, low and high, or middle and high).

In fact, the frequency of single layer occurrence in our database is very close to that found for the Cloud Layer Thickness Climatology (CLTC) presented in PWR95, where the frequency of occurrence of single-layer clouds at 63 sites (34 inland, 14 coastal and 15 island stations) in the Northern Hemisphere for 14 years (1975-1988) was analyzed. Cloud vertical structure (CVS) was determined from rawinsonde observations (RAOBS) of temperature and humidity and checked against (and sometimes combined with) surface weather observations (SWOBS). PWR95 found that over most sites the frequency of single-layer clouds was higher than 90%. However, they concluded that multilayered cases are underestimated in CLTC, when compared to another surface observation climatology, SOBS, from Hahn *et al.* (1982, 1984), which in turn seems to overestimate the multilayered occurrence.

Wang and Rossow (1995) performed also some statistical analysis on a database of cloud layers obtained from rawinsonde measurements taken at 30 oceanic or coastal stations. For the whole database, their method of cloud detection from the vertical profiles produced single layer cloud fields in only 60% of the cases, and about 26% corresponded to 2-layered conditions. Further, Wang *et al.* (1999) used various data sources from the Atlantic Stratocumulus Transition Experiment (ASTEX) including rawinsonde, radar, ceilometer, and satellite, to determine, among other features, the proportion between single and multi-layered conditions. They showed that the single layer frequency depends on the method of determination of the CVS. For the merged radar-ceilometer data (that is, using the ceilometer data to verify the radar-determined

lowest CBH), a single layer appeared 79% of cases, whereas the rawinsonde analysis gave only 52% of single layer cases. They also showed that single layers are more frequent for clouds below 3 km. In comparison, WRZ00 created a global CVS climatic dataset by analyzing a 20-year collection of twice-daily rawinsonde humidity profiles to estimate the height of cloud layers. They found that globally (for land and ocean profiles), 58% of clouds were single-layered and 42% multilayered, almost 67% of the latter being 2-layered clouds. Over land conditions they found 63% of single-layered structures, 27% of 2-layered systems, 7% of 3-layered, and 3% of systems with more than three layers.

Finally, global data from the study by Rossow and Zhang (2010) reveal that two satellite based systems, ISCCP in one hand and a combination of the CloudSat and CALIPSO (C&C) on the other hand, detected single cloud layers in 93.2% and 74.5% of the cases respectively, 2-layered systems in 6.3% and 18.0% of cases, and 3-layered systems 0.5% and 7.5% of the times. Note that C&C satellite combination is able to detect more multilayered situations because the powerfulness of their active (radar and lidar) instruments.

Therefore, our findings at Girona seem to confirm a tendency of ceilometers to overestimate the presence of single-layer cloud systems. The frequency of this kind of cloudiness according our measurements (89.7%) is almost the highest compared with the reviewed literature. There may be two reasons for such behavior: first, the effect of occultation by the first layer, which may hide other upper layers if it is thick enough, and second, the limited range reached by the ceilometer, so the highest clouds are not detected at all. These two limitations are further discussed in Section 3.5.

3.3 CBH distributions

Figure 2 shows the frequency distributions of CBH retrieved with the ceilometer for the whole analyzed period. All histograms have been standardized (by dividing each absolute frequency by the total number of values for the analyzed period) in order to better comparing their shapes. The bins are 400 m wide, thus leading to 20 intervals in the total detection range of the ceilometer (0 to 7620 m, so the last bin corresponds to a width of only 20 m). In Figure 2a the distribution of CBH for all cases together (i.e. single-, two- and three- layered conditions) is presented, in comparison with the CBH distribution for cases with a single layer detected. As these single-layered cases represent near the 90% of the total, both distributions are very similar. Figures 2b and 2c show the CBH distributions for 2-layered and 3-layered systems respectively.

The histogram for all CBH together (Figure 2a) has the maximum for the bin centered at 1400 m (for the single-layered systems, the maximum is found for the bins centered at 1000 and 1400 m) and shows a progressive decreasing frequency up to the maximum level of detection of the ceilometer. Low clouds (below 2000 m) represent 49.6% of detected CBH (52% of single-layered systems), middle clouds (2000-6000 m) are the 42.9%, and high clouds (> 6000 m), the 7.5%. Combining the frequency of low clouds with the cloud occurrence specified in section 2.1 (40-50%), we can derive an approximately low cloud occurrence (25.7%) that agrees with the low cloud cover obtained from visual observations (i.e., from the already mentioned SYNOP observations at Girona Airport).

The mean and median of the distribution for all CBH together are 2559 m and 1973 m respectively, whereas for the single-layered systems these values are 2582 m and 1983 m. The mean of the distribution agrees well with WRZ00, who found that the

CBH global average was at 2.4 km, being averaged CBH higher for land (2.8 km) than for ocean stations. Likewise, in PWR95, where the CLTC dataset was used, the latitudinal dependence of the averaged CBH is presented; according with their results (for land and latitudes near 42°), averaged CBH is around 2.4 km. For the WR95 dataset (which includes only stations that represent oceanic climatology), cloud bases are located 57% of the time below 2 km, with an even distribution above 2 km and a mean value of 2.6 km, so again very close to the mean value retrieved at Girona from our ceilometer measurements.

Despite this agreement with averaged values, the histogram (Figure 2a) shows some differences when compared with previous published results. For example, the histogram shown in WRZ00, both for land and ocean cases, is very biased to low CBH: about one-third of clouds have CBH below 0.5 km, with a sharp decrease of frequencies up to 1 km, followed by a smoother decrease above 2 km. Contrarily, the CBH distribution observed in Girona (with a clear maximum at 1400 m) is remarkably more similar to that in WR95, although this latter histogram has a much more peaked shape, with the maximum of the distribution centered at 1000 m. This could be explained by the fact that in WR95 all 30 stations were located at oceanic places, thus with a dominant contribution of low stratiform layers (marine *Stratocumulus*). Again, when comparing our results with WRUR99, several differences appear (dominant frequency for clouds below 2 km, and the peak of the distribution at around 700 m) owing to the fact that the focus of that study was put on marine boundary layer clouds.

Other authors have analyzed the vertical distribution of clouds observed at different locations by a suite of ground-based instruments (Mace and Benson, 2008; Ebell *et al.*, 2011; Morcrette *et al.* 2012; Qian *et al.*, 2005) or estimated by Global

Circulation Models (Illingworth *et al.*, 2007). All of them use the probability to find a cloud in a given level of the atmosphere, which is not directly and rigorously comparable with the frequency distribution of the CBH measured by the ceilometer. In any case, these works show an accumulation of cloudiness at approximately 1-2 km and a second maximum at higher altitudes (8-9 km), which again indicates a lower presence of high clouds when observed by the ceilometer when compared with other methods (e.g. MMCR, ARSCL, RS, models).

The distribution of CBH for 2-layered systems is shown in Figure 2b. For the lower layer, 70% of the retrieved CBH is below 3000 m. Strictly speaking, the maximum of the distribution is for the bin centered at 600 m, though high frequencies extend towards considerably higher CBH; the mean (median) of this distribution is 2403 m (1975 m). The upper layer detected with the ceilometer shows a bimodal distribution that has the main maximum for the bin centered at 1800 m, though appreciable frequencies extend also towards much higher values reaching the detection limit of the ceilometer (secondary maximum at 3400 m; mean and median are 3249 m and 3048 m respectively). These retrievals can be compared with the statistics for 2-layered systems in WR00, where the averaged CBH for the lower layer (for land stations) is 1.1 km, while average for the upper layer is 4.8 km.

Figure 2c shows the distributions of CBH for 3-layered systems as detected by the ceilometer. The distribution of the CBH for the lowest layer shows a maximum around 1000 m; for the middle layer, the distribution is bi-modal (with maxima at 1800 and 3400 m); the distribution for the highest layer has a peak around 3800 m and a secondary maximum at 2200 m. The mean (median) of the three distributions are 2054 m (1817 m), 2827 m (2693 m), and 3553 m (3478 m). Wang *et al.* (2000),

regarding 3-layered cloud systems found the corresponding CBH averages at 0.8 km, 2.9 km and 5.5 km for land sites. The comparison of the latter results with ours seems to confirm that the derived CVS depends upon the detection system (radiosonde and ceilometer).

For multilayered cloud systems, distances between CBH of adjacent layers can be seen in Figure 3. The mean (median) of the distribution of CBH distances for 2-layered systems is 846 m (1074 m). When three layers are detected, the mean (median) distance between the lowest CBH and the middle CBH is 773 m (876 m), and between the middle and the highest CBH, 726 m (785 m). These values are quite different from separation between layers reported by WR95 (mean separation of 2.1 km, although most cases have separation between 0.5 and 1 km) and by WRZ00 (mean separation of 2.2 km and 2.3 km over ocean and land respectively). Therefore, important differences between methods used for finding the CBH arise again, considering that the latter values correspond to depth of clear air between adjacent cloud layers while our findings are distances between cloud bases.

As it has been previously stressed, ceilometers have difficulties retrieving a second layer over a thick first layer, which add to the inability to determine the cloud top and the limited range of detection. On its side, CVS estimation from radiosonde profiles may have also its own limitations, starting from the difficulty of establishing humidity and temperature thresholds. Moreover, Chernykh and Aldukhov (2004) pointed out that the profile resolution could produce some errors in the gradient calculation that form part of the cloud determination. In addition, deficits in spatial (i.e. lack of data of some parts of the World) and temporal (i.e., soundings are launched two

times per day) hinder the broad use of sounding vertical profiles for climatic studies of cloud vertical structure (Poore *et al.* 1995; Nowak, 2008).

3.4. Yearly evolution of the CBH distribution

Figure 4 shows the retrieved monthly distributions of CBH for single layer cases, for some representative months (January, April, July and October, i.e. the central month of every season), to figure out how CBH distribution evolves through the year. The remaining months have also been treated, but they are not included in the figure for the sake of simplicity. In general, the monthly histograms show some common features: distributions are often multimodal, and frequencies decrease for high clouds. Despite these common characteristics, an evolution along the year appears clearly in Figure 4. January histograms are representative of the relatively homogeneous distributions for winter months, and have the maximum at the bin centered at 1000 m (January 2007 has a marked second maximum at 5800 m). In April, histograms have a more compact shape, with the maximum ranging from 800 to 2400 m, except for the high contribution of very low clouds (with CBH < 400 m) in April 2007. In July (note that distributions for the four years are very similar) low clouds dominate again, with a much more peaked maximum always centered at 1400 m, possibly due to the predominantly anticyclonic and barometric swamp weather types, that favors the appearance of daily evolution clouds, and the eventual passing of weather fronts, both conditions favoring the accumulation of the CBH in low values. Finally, in October, the maxima of the distributions, which are less marked, extend from 400 m (for year 2010) to 1600 m (there is a second maximum centered at 3000 m in year 2007).

Another way to make evident the seasonal evolution of the CBH distribution throughout the year is using cumulative CBH frequencies. Figure 5a presents all

Januaries and Julies from 2007 to 2010 whereas 5b presents Aprils and Octobers. It can be seen that Januaries and Julies are quite different since these months correspond to extreme seasons, whereas Aprils and Octobers are more similar, due to the fact that both correspond to transitional (equinoctial) seasons. Finally, Figure 5c shows the mean of the cumulative CBH frequencies for January, April, July and October, from 2007 to 2010, all together. All these figures show that, in July, there are (relative to the other months) few cases (25%) with CBH less than 1400 m, but 80% of clouds are below 3000 m. Contrarily, in January almost 40% of detected clouds have CBH less than 1000 m, so clouds up to 5000 m have to be accounted to reach 80% of cases. As already mentioned, the equinoctial seasons lay between these two extreme behaviors.

The asymmetry and “peakedness” of the histograms (i.e. their shape) can be described through the skewness and kurtosis parameters respectively, which correspond to the third and fourth moments with respect to the mean of the CBH frequency distributions. For the CBH distributions, skewness is always positive (which means that the right tail is more pronounced than the left tail) and presents a high negative correlation ($r^2 = 0.83$, p-value < 0.0001) with the mean; while it is highly correlated ($r^2 = 0.83$, p-value < 0.0001) with kurtosis. This means that distributions with a low mean CBH are very asymmetric having the tails biased to high values and show high peakedness (large kurtosis values). The best example is July, which presents large kurtosis and asymmetry values. These characteristics for July are probably due to the contribution of convective clouds to high frequencies of low clouds, as already commented in previous sections. In other seasons, the origin of clouds is more diverse (including a large contribution of clouds associated to low pressure systems and their fronts) so cloud base heights are distributed along the histograms.

3.5. CBH behavior during some atmospheric situations

In this section we explain three typical cloudiness situations as seen by the ceilometer, and discuss their contribution to the frequency distributions of CBH. One case for winter and two cases for summer are shown, as examples of expected conditions in these seasons. Most winter cloudiness is related with synoptic situations, and more specifically, with fronts that cross the area (see section 3.5.1); in addition, there are fogs and some very low clouds (*Stratocumulus*, *Stratus*) related with local stability conditions below the subsidence thermal inversion associated to high pressure systems. On the other hand, in summer (section 3.5.2) there is cloudiness associated to synoptic situations (fronts crossing over the region) like in winter, but there is also another source of cloudiness: the surface heating and the subsequent convection that produces low clouds (*Cumulus humilis*) almost daily.

3.5.1 Winter low pressure systems

The jet stream in winter usually adopts a zonal configuration, which allows a continuous western flux at the site latitude. This was the synoptic situation from 21 to 31 December 2009, when there was an episode of continued low pressure systems crossing the Iberian Peninsula from southwest to northeast. The weather fronts had lost power when arrived in the north-east of the peninsula, but they still left some precipitation over Girona (17.8 mm along these 11 days, according the rain gauge at the meteorological station placed side-by-side with the ceilometer). Figure 6a shows the CBH ceilometer data for the whole month. Between days 21 and 31 clouds formed along weather fronts and appeared day by day in an almost periodic way. During these days, there are first high and middle level clouds, from the maximum vertical range of the ceilometer going down towards the level of low clouds, but more often in the 4000-

6000 m range. Then, when clouds reach low level (less than 2000 m) they remain at this level for several hours (6-12 h), and produce rainfall in most cases when the front overpasses the site (probably associated to the presence of *Nimbostratus*). Few hours after such an evolution of clouds, the sequence is repeated again. As the ceilometer detects CBH below 7620 m, the first, highest clouds that are expected with the arrival of a front (*Cirrus*, *Cirrocumulus*, *Cirrostratus*) cannot always be observed by this instrument. In addition, the highest clouds may appear when the low clouds are still present, and the latter may occult (both to an observer and to the ceilometer) the presence of the former. This can be seen for example in the transition between two consecutive systems the night of December 25 (Figure 6b, between 18 and 24 h): a layer of high-middle clouds (starting at CBH > 6000 m and descending to CBH < 4000 m) is apparent and occasionally detected by the ceilometer through the lower layer (CBH at 1000-2000 m).

Figure 6b corresponds to a detail for days 25 and 26 December 2009 and shows a particular example of a two consecutive low pressure systems. In fact, the synoptic maps of these two days (e.g. <http://www.met.fu-berlin.de/de/wetter/maps/>) show the successive cold fronts and an occluded warm front. According to the weather type classification by Martin-Vide (2005), conditions change from a Northwest advection on day 25 to a South-Southeast advection on day 26, due to the changing position of the low pressure system center. The typical evolution of clouds and the descending CBH, as described above, is clearly detected by the ceilometer. Rain can also be observed in ceilometer plots, starting on day 26 at 5:25. On day 25, the hemispheric camera images (only for daylight hours, that is from 7:30 to 16:00 UTC approximately) show sometimes a clear sky (Fig. 6i) but most time dominated by broken *Stratocumulus* clouds (Fig. 6ii). On day 26, clouds (mainly *Stratus*) totally cover the sky; these clouds

sometimes show some vertical structure, so the ceilometer reports the cloud base at variable altitudes or even detects more than one layer (see Fig. 6b, at around noontime, and Fig. 6iii).

Figure 7 shows the CBH frequency distribution for the period 21-31 December 2009, i.e., the period above described as an example of continuous front crossing. Thus, it is obvious that when fronts are passing, CBH is concentrated either at low altitudes or at middle levels. In fact, the distribution has two maxima, at 1000 m and 5000 m. Figure 7 also shows the CBH distribution for the short period (25-26 December 2009). The two histograms are bimodal, but the CBH distribution for the longer period is more uniform than the distribution for days 25-26, which has a much higher peak for low clouds (maximum at 1400 m). The reason is that not all the fronts of the longer period produced low level clouds as the passing fronts on the 25-26 did. For instance, on the 28-29 only few clouds reach the lower heights. On the other hand, the period previous to the start of the passing fronts shows a great variability of CBH, including some days with no clouds. All these facts contribute to make the histogram for the whole month (not shown) relatively uniform, as we have seen for winter months (section 3.4, Figure 4).

3.5.2 Summer conditions

Figure 8a shows the CBH detected by the ceilometer in July 2009. From July 4-7, 2009, and according to the weather reports from the Meteorological Service of Catalonia, a low pressure system arrived in the area and made the temperature to cool down and the atmosphere to progressively unstabilize. Specifically, on July 6 the weather front crossed over the site and left a very weak precipitation persisting until the next day; this can be seen in Figure 8b, where the detail of the ceilometer CBH detected

for the period 6-7 July 2009 is shown. The typical evolution of clouds associated to a low pressure system (i.e., as above commented for a winter case) is clear, in particular from the later hours on day 6. Nevertheless, this summer cold front episode behaves slightly different, since low clouds stay longer than its winter counterparts shown in section 3.5.1. The sky camera images for day 7 confirm the evolution from high clouds to low thick clouds that remain over the site after noon (Fig. 8i and 8ii).

Other summer days show a very different behavior regarding cloudiness. For example, Figure 8a indicates that some days have mainly low level clouds, and only during a part of the day (days 12, 13, 18, 19, 30, 31). As an example of this characteristic evolution, Figure 8c shows the CBH for days 18-19 July 2009. This behavior, with low clouds appearing around noon, is typical of convective clouds of daily evolution: the surface heating and subsequent free convection forms low clouds, more specifically *Cumulus humilis* (fair weather clouds), which indicate warm weather, frequent in Girona summertime. The analyses of the synoptic maps for those days confirm that conditions were favorable to convection: a slight Northwest advection on day 18 and a barometric swamp on day 19, with a trough in the south of Iberian Peninsula (classification from Martin-Vide, 2005). Moreover, the vertical profile obtained by radiosonde in Barcelona (90 km south of Girona) corroborates free convection conditions: the bulk Richardson number between 0 and 500 m a.g.l. at noontime is -2.7 and -10.7 respectively for days 18 and 19, due to super-adiabatic conditions and weak winds. In addition, *Cumulus* clouds are continuously forming and disappearing (Fig. 8iii and 8iv) within the field of view of the hemispheric sky camera. Some thin, high clouds (not seen by the ceilometer) seem to be present on day 19 (Fig. 8iv), enhancing circumsolar radiation which is seen as a white circle in the image.

The frequency distributions of CBH for these two different summer conditions (6-7 July and 18-19 July) are shown in Figure 9. Both histograms have marked peaks for low clouds. For the low pressure system, the maximum is at 1400 m, with a secondary maximum at 3400 m, although there are clouds at almost all altitudes during the whole episode. For the convective situation, clouds for both days concentrate their bases within the bin centered at 1400 m, despite of some slightly higher clouds (bin centered at 2200 m) before noon of day 18. A more detailed analysis of this situation indicates that the mean CBH for the lowest layer was 1768 m (1504 m) for July 18 (July 19). This is in agreement with the lifting condensation levels, that according to surface conditions at the site (at noontime) was somewhat higher (1700 m) for day 18 than for day 19 (1200 m). In summary, both situations accumulate higher frequencies of CBH at low levels, in particular at 1400 m, where the two distributions have the maximum, contributing to the peakedness of CBH distributions for July (see Fig. 4).

4. Conclusions

For the considered database of high resolution (both in time, four years of 12 s measurements; and in the vertical direction, 10 m) ceilometer measurements taken at Girona within the period 2007-2010, the monthly cloud occurrence follows a similar evolution along the four years. Cloud occurrence has an average value about 40-50%, with a summer minimum (down to 30%) centered in July. This behavior is also found in local climatology based on visual observations, despite the different field of view associated to each methodology, and also despite the shortness (from the climatic point of view) of our dataset. Moreover, these results are consistent with regional climatology based on surface and satellite observations.

The cloud vertical structure has also been analyzed from the same dataset. The proportion of single layer cases, about 90%, is clearly an overestimation, linked to the missing very high layers (above 7620 m, the range limit of our ceilometer) and to undetected layers above the lowest layer present. Comparison with other studies from the literature confirms this preferential assignation to single layer cases.

Monthly CBH distributions show a yearly cycle with more uniform or bimodal distributions in winter (therefore with lower skewness) and peaked distributions (higher kurtosis) in summer. The particular behavior of cloudiness in summer is represented by the CBH distributions in July, which are clearly peaked at the bin centered at 1400 m. Low clouds originated from synoptic conditions on the one hand and from local convective activity on the other hand can contribute to this accumulation. The seasonal evolution is confirmed by the cumulative frequencies for the CBH: in July, only 25% of cases have CBH less than 1400 m, but 80% of clouds are below 3000 m. Contrarily, in

January almost 40% of detected clouds have CBH less than 1000 m, so clouds up to 5000 m have to be accounted to reach 80% of cases.

Despite the limited temporal extension of the ceilometer database used and that only measurements from one location (Girona) have been used, some features that may be common to all ceilometer systems have been found. First, our ceilometer has confirmed its ability to operate throughout the year taking continuous measurements of the lowest CBH. In addition, we have found that the estimations of average cloud cover for long periods (months, years) are reasonably good, and that the retrieved CBH distributions are, at least for single-layered cloud field structures, similar to those found using other methodologies. As expected, the ceilometer cannot provide a complete description of the CVS (that is, cloud tops and the number of cloud layers actually present) in multilayered conditions, given their inherent limitations (limited range, obscured upper layers). In fact, our results indicate –as other authors have already pointed out- that ceilometers might be quite imperfect when describing these systems (i.e., with the presence of either both low and middle clouds, or both low and high clouds, for example). The use of ceilometers with a larger range of detection (as the CL51 from Vaisala, or the CHM15k from Jenoptik, Martucci *et al.* (2010)) improves the CBH distributions retrieved, but only synergetic observations with other active instruments (cloud radar) would produce a more reliable statistics of cloud vertical structure.

The results obtained, however, are sufficiently encouraging to assume that ceilometers may become a complement or even a replacement of human observations, at least for the average cloud occurrence for relatively long periods (months). It would be recommendable to update a deep comparison between ceilometer measurements and

radiosonde estimation methods for detecting clouds (and their CBH and CVS). Such a comparison could be more comprehensive if a top-down view (i.e. satellite information) were added to describe the highest clouds. The specific algorithm that obtains CBH from the backscatter signal could be improved for detection of upper layers, although we recognize that the signal extinction in the lowest layer may be difficult to overcome. The statistical analysis applied in the present work could be used to further describe cloud characteristics of extended (temporally or spatially, i.e. with similar databases from other sites) or improved (i.e., higher detection range, better multilayer detection) datasets containing ceilometer measurements.

Acknowledgments

This research was funded by the *Ministerio de Ciencia e Innovación* of the Spanish Government through grants CGL2007-62664 (NUCLIEREX) and CGL2010-18546 (NUCLIERSOL) projects. Visual observations of cloudiness used for comparison have been kindly provided by the Spanish *Agencia Estatal de Meteorología* (AEMET). Montse Costa-Surós was supported by research fellowship FPI BES-2008-003129 from *Ministerio de Ciencia e Innovación* of the Spanish Government. The authors would like to express their gratitude to reviewers for the valuable suggestions that allowed to improve the paper.

References

- Boers, R., de Haij, M., Wauben, W., Baltink, H., van Ulf, L., Savenije, M., Long, C.N., 2010. Optimized fractional cloudiness determination from five ground-based remote sensing techniques. *J. Geophys. Res.* 115, 1-16.
- Calbó, J., Sanchez-Lorenzo, A., 2009. Cloudiness climatology in the Iberian Peninsula from three global gridded datasets (ISCCP, CRU TS 2.1, ERA-40). *Theor. Appl. Climatol.* 96, 105-115.
- Chernykh, I., Aldukhov, O., 2004. Vertical distribution of cloud layers from atmospheric radiosounding data. *Izv. Atmos. Ocean. Phys.* 40, 41-53.
- Clothiaux, E., Ackerman, T., Mace, G., Moran, K., Marchand, R., Miller, M., 2000. Objective determination of cloud heights and radar reflectivities using a combination of active remote sensors at the ARM CART sites. *J. Appl. Meteorol.* 39, 645-665.
- Dai, A., Karl, T., Sun, B., Trenberth, K., 2006. Recent trends in cloudiness over the United States - A tale of monitoring inadequacies. *Bull. Am. Meteorol. Soc.* 87, 597-606.
- de Leeuw, G., Kokhanovsky, A., Cermak, J., 2012. Remote sensing of aerosols and clouds: Techniques and applications (editorial to special issue in *Atmospheric Research*). *Atmos. Res.* 113, 40-42.

- Ebell, K., Crewell, S., Loehnert, U., Turner, D.D., O'Connor, E.J., 2011. Cloud statistics and cloud radiative effect for a low-mountain site. *Q. J. R. Meteorol. Soc.* 137, 306-324.
- Eberhard, W.L., 1986. Cloud Signals from Lidar and Rotating Beam Ceilometer Compared with Pilot Ceilig. *J. Atmos. Ocean. Technol.* 3, 499-512.
- Feister, U., Moeller, H., Sattler, T., Shields, J., Goersdorf, U., 2010. Comparison of macroscopic cloud data from ground-based measurements using VIS/NIR and IR instruments at Lindenberg, Germany. *Atmos. Res.* 96, 395-407.
- Forsythe, J., Haar, T.V., Reinke, D., 2000. Cloud-base height estimates using a combination of meteorological satellite imagery and surface reports. *J. Appl. Meteorol.* 39, 2336-2347.
- Hahn, C.J., Warren, S.J., London, J., Chervin R.M., Jenne, R., 1982. Atlas of Simultaneous Occurrence of Different Cloud Types over the Ocean. NCAR Tech., Boulder.
- Hahn, C.J., Warren, S.J., London, J., Chervin R.M., Jenne, R., 1984: Atlas of Simultaneous Occurrence of Different Cloud Types over Land. NCAR Tech., Boulder.
- Heintzenberg, J., Charlson, R.J., 2009. Clouds in the perturbed climate system: their relationship to energy balance, atmospheric dynamics, and precipitation. The MIT Press, Cambridge.

- Henderson-Sellers, A., 1992. Continental cloudiness changes this century. *Geophys. J.* 27, 255-262.
- Hogan, R., Francis, P., Flentje, H., Illingworth, A., Quante, M., 2003. Characteristics of mixed-phase clouds. I: Lidar, radar and aircraft observations from CLARE'98. *Q. J. R. Meteorol. Soc.* 129, 2089-2116.
- Hogan, R., O'Connor, E., Illingworth, A., 2009. Verification of cloud-fraction forecasts. *Q. J. R. Meteorol. Soc.* 135, 1494-1511.
- Holejko, K., Nowak, R., 2000. Continuous wave laser ceilometer with code modulation for measurements of cloud base height. *Opto-Electron. Rev.* 8, 195-199.
- Hwang, P., Stowe, L., Yeh, H., Kyle, H., 1988. The Nimbus-7 Global Cloud Climatology. *Bull. Am. Meteorol. Soc.* 69, 743-752.
- Illingworth, A., Hogan, R., O'Connor, E., Bouniol, D., Brooks, M., Delanoe, J., 2007. Cloudnet - Continuous evaluation of cloud profiles in seven operational models using ground-based observations. *Bull. Am. Meteorol. Soc.* 88, 883.
- Jin, X., Hanesiak, J., Barber, D., 2007. Detecting cloud vertical structures from radiosondes and MODIS over Arctic first-year sea ice. *Atmos. Res.* 83, 64-76.
- Jones, D.W., Ouldridge, M., Painting, D.J., 1988. WMO International Ceilometer intercomparison: final report. WMO, United Kingdom.
- Kotarba, A., 2009. A comparison of MODIS-derived cloud amount with visual surface observations. *Atmos. Res.* 92, 522-530.

- Kaiser, D.P., 2000. Decreasing cloudiness over China: An updated analysis examining additional variables. *Geophys. Res. Lett.* 27, 2193-2196.
- L'Ecuyer, T., Jiang, J., 2010. Touring the atmosphere aboard the A-Train. *Phys. Today.* 63, 36-41.
- Llach, M., Calbó, J., 2004. Aproximación a la Climatología de la nubosidad en Cataluña, in: García Cordon, J.C., Diego Liaño, C., Fernández Arróyabe Hernández, P., Garmendia Pedraja, C., Rasilla Álvarez, D. (Eds.), *El Clima, entre el mar y la montaña.* Asociación Española de Climatología, Santander, pp. 325-334.
- Long, C., Sabburg, J., Calbó, J., Pages, D., 2006. Retrieving cloud characteristics from ground-based daytime color all-sky images. *J. Atmos. Ocean. Technol.* 23, 633-652.
- Mace, G., Benson, S., 2008. The vertical structure of cloud occurrence and radiative forcing at the SGP ARM site as revealed by 8 years of continuous data. *J. Clim.* 21, 2591-2610.
- Mancuso, R.L., Serebreny, S.M., Blackmer, R.H.J., 1971. A Cloud Simulation Model for Evaluating Automatic Ceilometer Systems. *J. Appl. Meteorol. Climatol.* 10, 1324-1330.
- Martin-Vide, J., 2005. Catálogo de situaciones sinópticas. Los mapas del tiempo. Ed. Davinci, 63-67.

- Martucci, G., Milroy, C., O'Dowd, C., 2010. Detection of Cloud-Base Height Using Jenoptik CHM15K and Vaisala CL31 Ceilometers. *J. Atmos. Ocean. Technol.* 27, 305-318.
- Moran, K., Martner, B., Post, M., Kropfli, R., Welsh, D., 1998. An unattended cloud-profiling radar for use in climate research. *Bull. Am. Meteorol. Soc.* 79, 443-455.
- Morcrette, C.J., O'Connor, E.J., Petch, J.C., 2012. Evaluation of two cloud parametrization schemes using ARM and Cloud-Net observations. *Q. J. R. Meteorol. Soc.* 138, 964-979.
- Münkel, C., Eresmaa, N., Rasanen, J., Karppinen, A., 2007. Retrieval of mixing height and dust concentration with lidar ceilometer. *Boundary-Layer Meteorol.* 124, 117-128.
- Nowak, D., Ruffieux, D., Agnew, J., Vuilleumier, L., 2008. Detection of fog and low cloud boundaries with ground-based remote sensing systems. *J. Atmos. Ocean. Technol.* 25, 1357-1368.
- Poore, K., Wang, J., Rossow, W., 1995. Cloud Layer Thicknesses from a Combination of Surface and Upper-Air Observations. *J. Clim.* 8, 550-568.
- Probst, P., Rizzi, R., Tosi, E., Lucarini, V., Maestri, T., 2012. Total cloud cover from satellite observations and climate models. *Atmos. Res.* 107, 161-170.
- Qian, Y., Long, C.N., Wang, H., Comstock, J.M., McFarlane, S.A., Xie, S., 2012. Evaluation of cloud fraction and its radiative effect simulated by IPCC AR4

global models against ARM surface observations. *Atmos. Chem. Phys.* 12, 1785-1810.

Ramanathan, V., Cess, R., Harrison, E., Minnis, P., Barkstrom, B., Ahmad, E., 1989. Cloud-Radiative Forcing and Climate: Results from the Earth Radiation Budget Experiment. *Science*. 243, 57-63.

Rossow, W., Schiffer, R., 1991. ISCCP Cloud Data Products. *Bull. Am. Meteorol. Soc.* 72, 2-20.

Rossow, W., Zhang, Y., Wang, J., 2005. A Statistical Model of Cloud Vertical Structure Based on Reconciling Cloud Layer Amounts Inferred from Satellites and Radiosonde Humidity Profiles. *J. Clim.* 18, 3587-3605. Salazar, J., Poveda, G., 2009. Role of a simplified hydrological cycle and clouds in regulating the climate-biota system of Daisyworld. *Tellus Ser. B-Chem. Phys. Meteorol.* 61, 483-497.

Rossow, W.B., Zhang, Y., 2010. Evaluation of a Statistical Model of Cloud Vertical Structure Using Combined CloudSat and CALIPSO Cloud Layer Profiles. *J. Clim.* 23, 6641-6653.

Schroeder, M., Ament, F., Chaboureau, J., Crewell, S., 2006. Model predicted low-level cloud parameters Part II: Comparison with satellite remote sensing observations during the BALTEX Bridge Campaigns. *Atmos. Res.* 82, 83-101.

Solomon, S., Qin, D., Manning, M., Alley, R.B., Berntsen, T., Bindoff, N.L., Chen, Z., Chidthaisong, A., Gregory, J.M., Hegerl, G.C., Heimann, M., Hewitson, B., Hoskins, B.J., Joos, F., Jouzel, J., Kattsov, V., Lohmann, U., Matsuno, T., Molina, M., Nicholls, N., Overpeck, J., Raga, G., Ramaswamy, V., Ren, J., Rusticucci, M.,

- Somerville, R., Stocker, T.F., Whetton, P., Wood R.A., Wratt, D., 2007. Technical Summary. *Climate Change 2007: The Physical Science Basis. Contribution of Working Group I to the Fourth Assessment Report of the Intergovernmental Panel on Climate change* (Eds. Solomon, S., Qin D., Manning, M., Chen, Z., Marquis, M., Averyt, K.B., Tignor, M., Miller, H.L.). Cambridge University Press, Cambridge, United Kingdom and New York, 21-88.
- Sun, B., Groisman, P.Y., 2000. Cloudiness variations over the Former Soviet Union. *Int. J. Climatol.*, 20, 1097-1111.
- van Lipzig, N.P.M., Schroeder, M., Crewell, S., Ament, F., Chaboureau, J., 2006. Model predicted low-level cloud parameters - Part I: Comparison with observations from the BALTEX Bridge Campaigns. *Atmos. Res.* 82, 55-82.
- Wang, J., Rossow, W., Zhang, Y., 2000. Cloud vertical structure and its variations from a 20-yr global rawinsonde dataset. *J. Clim.* 13, 3041-3056.
- Wang, J., Rossow, W., Uttal, T., Rozendaal, M., 1999. Variability of cloud vertical structure during ASTEX observed from a combination of rawinsonde, radar, ceilometer, and satellite. *Mon. Weather Rev.* 127, 2484-2502.
- Wang, J., Rossow, W., 1995. Determination of Cloud Vertical Structure from Upper-Air Observations. *J. Appl. Meteorol.* 34, 2243-2258.
- Warren, S.G., Hahn, C.J., 2002. Clouds: Climatology, in Holton, J.R., Curry, J.A. Pyle, J.A. (Eds.), *Encyclopedia of Atmospheric Sciences*, Academic Press, San Diego, pp. 476-483.

- Warren, S., Eastman, R., Hahn, C., 2007. A survey of changes in cloud cover and cloud types over land from surface observations, 1971-96. *J.Clim.* 20, 717-738.
- Wielicki, B., Cess, R., King, M., Randall, D., Harrison, E., 1995. Mission to Planet Earth: Role of Clouds and Radiation in Climate. *Bull. Am. Meteorol. Soc.* 76, 2125-2153.
- Willén, U., Crewell, S., Baltink, H., Sievers, O., 2005. Assessing model predicted vertical cloud structure and cloud overlap with radar and lidar ceilometer observations for the Baltex Bridge Campaign of CLIWA-NET. *Atmos. Res.* 75, 227-255.
- World Meteorological Organization, 2008. Guide of Meteorological Instruments and Methods of Observation. WMO. I & II, I.15-1 to I.15-11-II.2-10 to II.2-11.
- Zelinka, M., Hartmann, D., 2010. Why is longwave cloud feedback positive? *J. Geophys. Res.* 115, 1-16.

Figures:

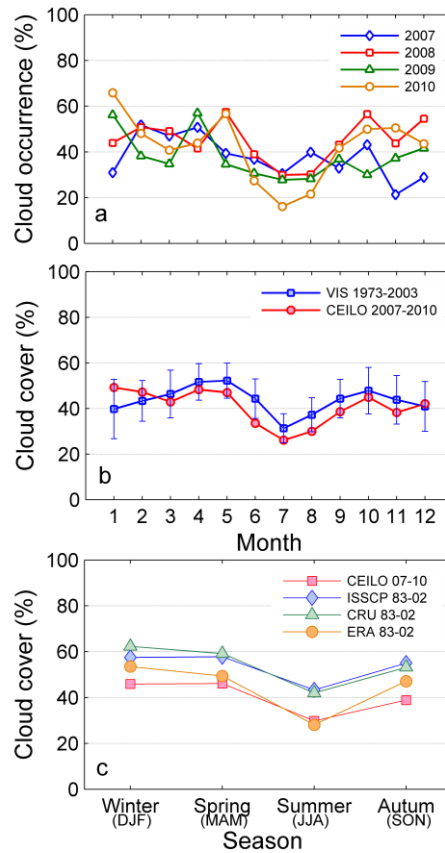


Figure 1. (a) Monthly cloud occurrence for the period 2007-2010, as derived from ceilometer data. (b) Averaged monthly cloud occurrence as detected by the ceilometer for the period 2007-2010 and averaged cloud cover from visual observations at Girona Airport for the period 1973-2003. Error bars indicate \pm one standard deviation, as an estimation of the interannual variability. (c) Seasonal cloud cover in the Iberian Peninsula, series from the ISCCP, CRU and ERA datasets (several periods, see Calbó and Sanchez-Lorenzo, 2009) and seasonal averages of cloud occurrence from ceilometer data.

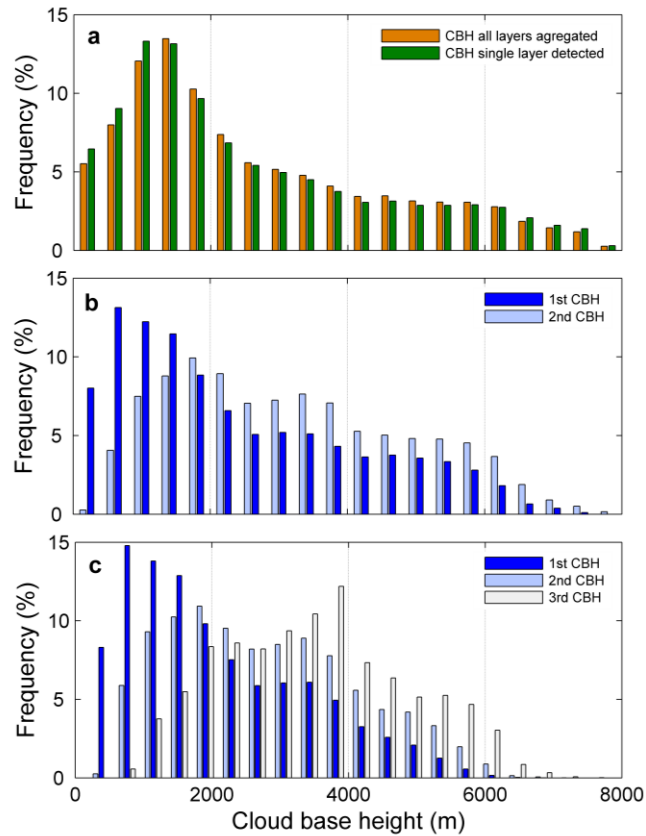


Figure 2. (a) Frequency distribution of CBH for all found layers aggregated, and when a single layer is detected. (b) Distribution of the CBH for the lower and higher layer when 2 layers are detected. (c) Distribution of the CBH for the lower, middle and higher layers when 3 layers are detected.

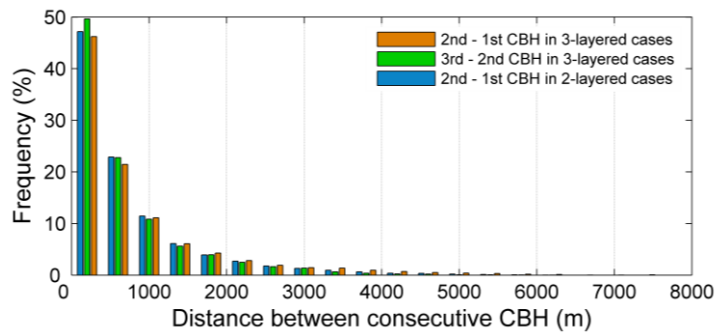


Figure 3. Frequency distribution of the distance between consecutive CBH detected by the ceilometer in multilayered cloud systems.

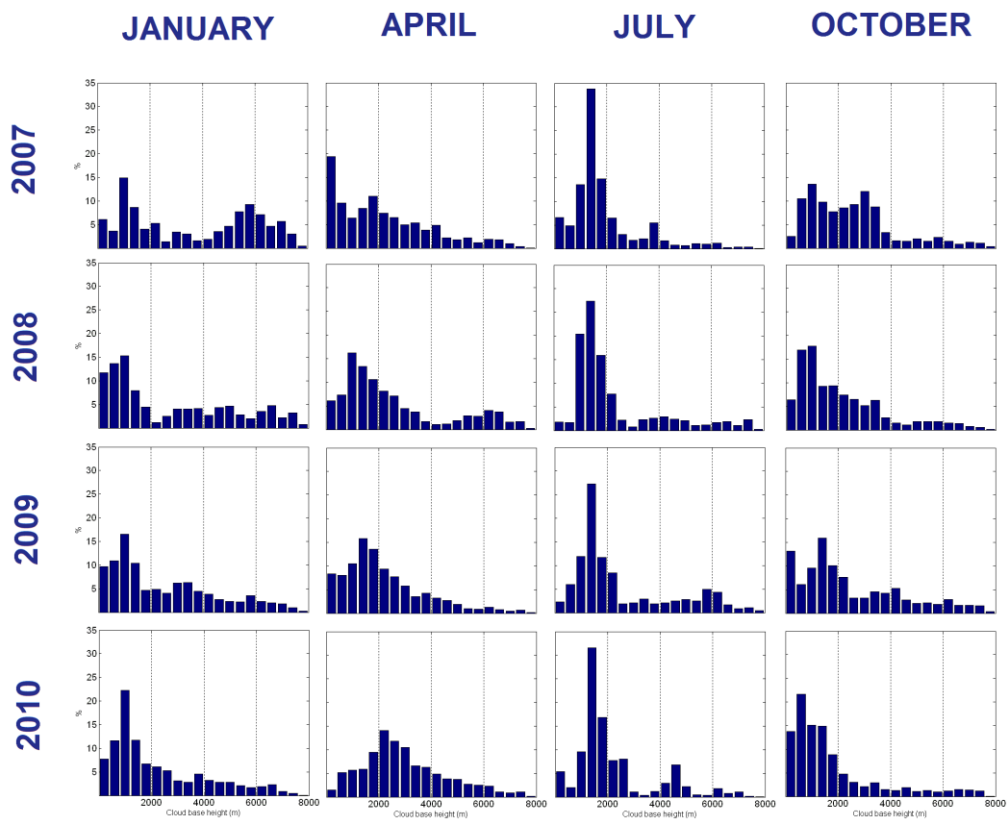


Figure 4. Standardized single layer CBH frequencies for some months, representative of each season, of the studied period.

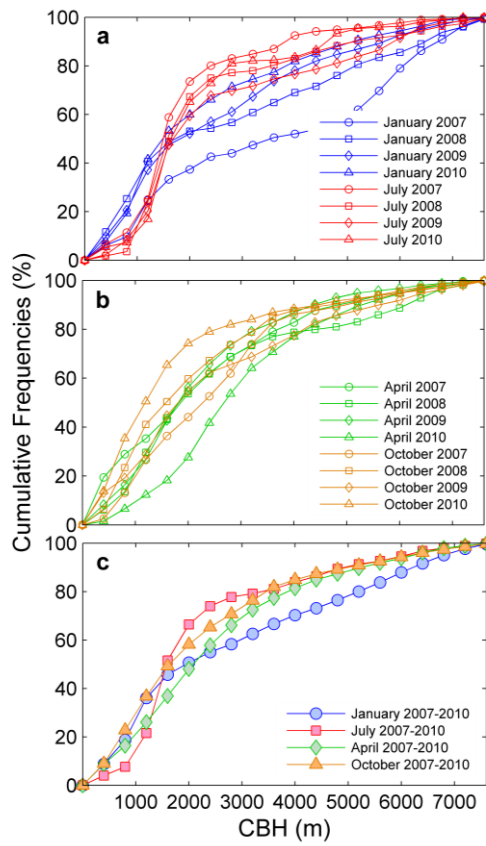


Figure 5. (a) January and July cumulative frequencies for the CBH of single layer cases; (b) April and October cumulative frequencies for the CBH of single layer cases; (c) Mean for the four years (2007-2010) cumulative frequencies for the CBH of single layer cases for January, April, July and October.

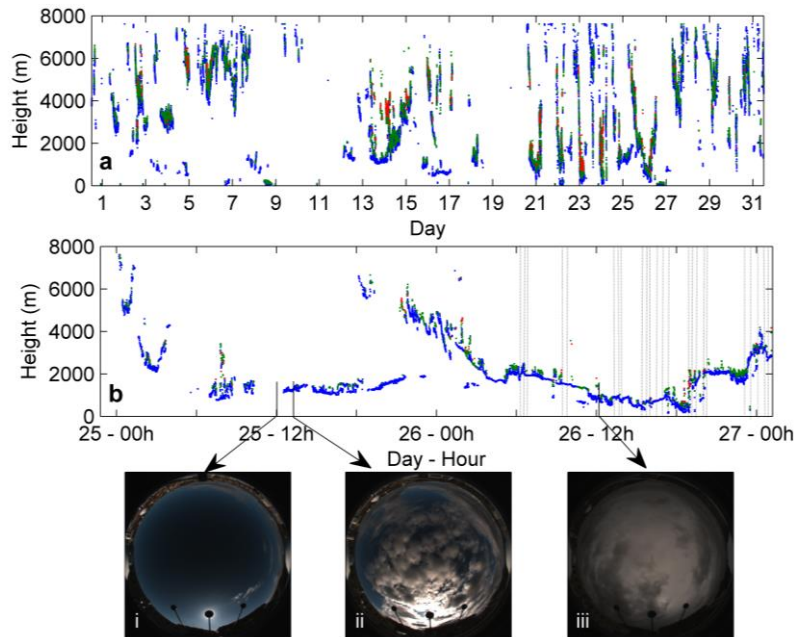


Figure 6. (a) Evolution of the ceilometer detected CBH in December 2009 (first CBH in blue, second CBH in green, third CBH in red). (b) A detail for 25-26 December 2009, including (dashed lines) the periods of rain, detected by the ceilometer itself and by the rain gauge and the sky camera. (i) Clear sky seen from the whole sky image from December, 25 at 12.00h. (ii) *Stratocumulus* clouds on December 25 at 12.45h. (iii) Sky image from December 26 at 12.06h where *Stratus* clouds cover all the sky and leave some precipitation.

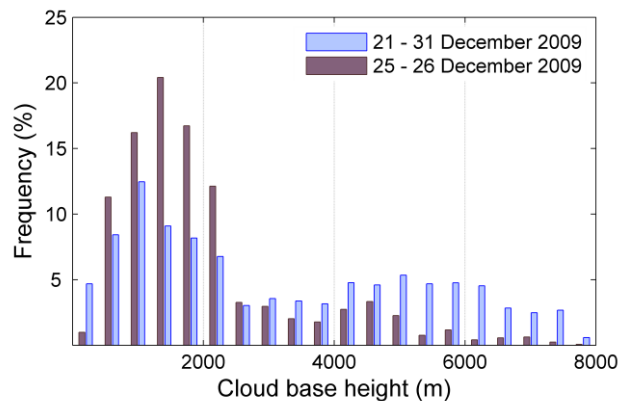


Figure 7. Frequency distributions of CBH for two different periods of December 2009.

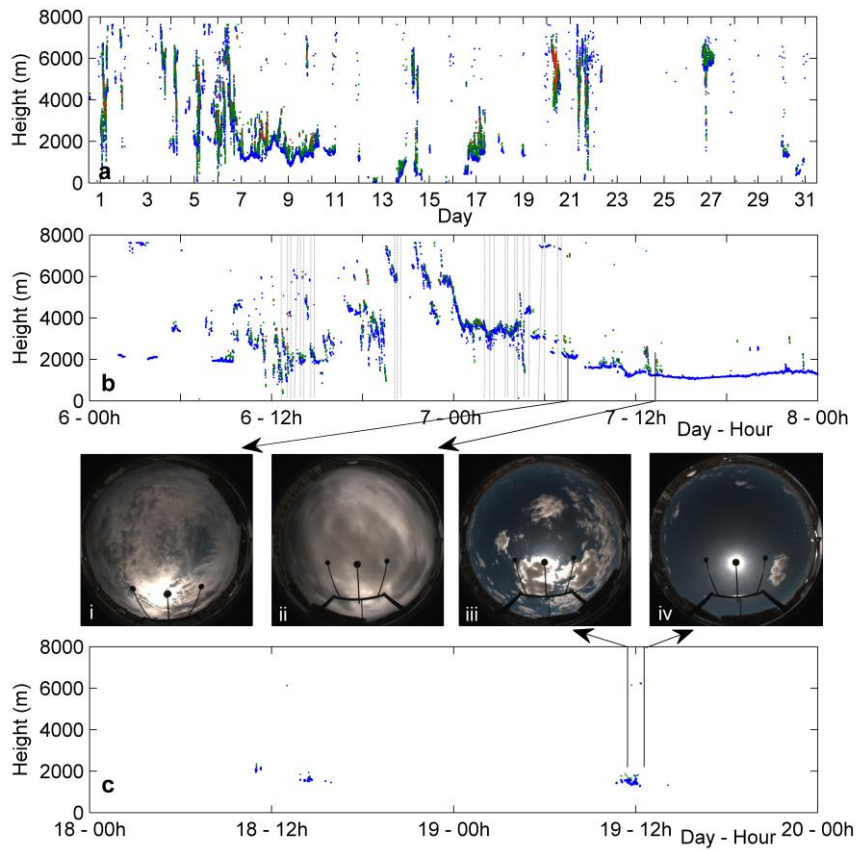


Figure 8. (a) Idem Fig. 6 but for July 2009. (b) A detail for 6-7 July 2009, including (dashed lines) the periods of rain. (i) Whole sky image from July 7 at 7.30h where several cloud types in different layers can be seen and (ii) at 13.15h with *Stratus* that cover the sky (c) A detail for 18-19 July 2009. (iii) Whole sky image from July 19 at 11.30h, with *Cumulus humilis* clouds produced by convection; (iv) the image taken at 12.30h where clouds are disappearing.

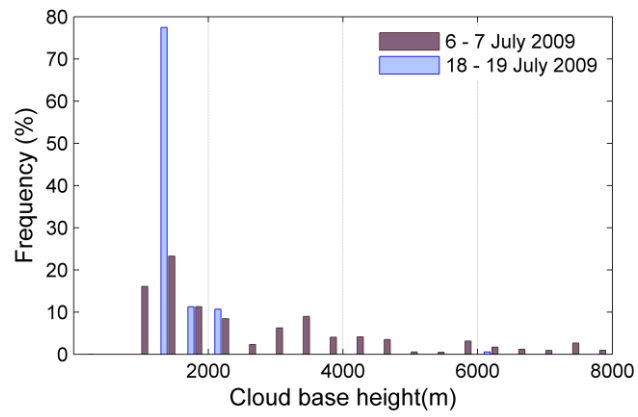


Figure 9. Frequency distributions of CBH for two different periods of July 2009.

Vitae:



Montse Costa-Surós (Girona, 1983) is a Ph.D. Student of the Experimental Sciences and Sustainability Program in the Group of Environmental Physics of the Physics Department at the University of Girona (UdG, Spain), and her Thesis is developed in the research frame of Clouds. She has a Degree in Environmental Sciences (Environmental Science and Technology field, 2005) and is Masters in Environmental Science (Environmental Physics and Technology itinerary, 2009) from the UdG. She did a research brief stay in the Pacific Northwest National Laboratory (WA, EUA) and in the company Vaisala (Finland), as part of her PhD Program formation.



Josep Calbó (Barcelona, 1965) has a degree in Physics from the University of Barcelona (1988) and a Ph.D. in Environmental Sciences from the Polytechnic University of Catalonia (1993). He has been a postdoctoral researcher at the Massachusetts Institute of Technology, and a visiting scientist at PNNL (USA), University of Southern Queensland (Australia) and NIWA (New Zealand). He is a member of the Environmental Physics Group and a professor in the Department of Physics at the University of Girona. In the context of the climate change, he focuses his research on radiation in the atmosphere, and interactions with clouds and aerosol.



Josep-Abel González (Ávila, 1962) is Ph.D. in Science for the Autonomous University of Barcelona (1989). Currently he is a Professor at the University of Girona (UdG), teaching Fundamentals of Physics in the Computer Engineering and Architecture studies. He also teaches Radiation and Remote Sensing in the Master in Environment. His scientific activities are devoted to various projects in the Environmental Physics Group of the University, covering the climatology of clouds and aerosol, their relation to radiation levels in the atmosphere, and the levels of ultraviolet radiation affecting plants and humans under various conditions.



Javier Martin-Vide (Barcelona, 1954) has a degree in Mathematics (University of Barcelona, 1977) and a Ph.D. in Geography and History (University of Barcelona, 1982). He is a Professor at the same university. He has been teaching from 1978 some Masters and Degree courses. He is an expertise in statistical analysis of daily precipitation, Synoptic Climatology, climatic change, urban climate and droughts in Iberian Peninsula. In 2011 he was nominated academician of the Royal Academy of Sciences and Arts of Barcelona and in 2012 corresponding academician of the Royal Academy of Overseas Sciences (Belgium). He is the president of the Association of the Spanish Geographers.